Am J Transl Res 2025;17(12):9478-9493
www.ajtr.org /ISSN:1943-8141/AJTR0162692

Original Article

Study on repair of periodontal bone defect in rats with PCL-PEG electrospun nanofibers combined with amniotic homogenate supernatant

Runan Wang[1*], Shun Yang[2*], Jiajia Cheng[1], Ni Wang[2], Guangsheng Chen[2], Qi Liu[2], Kun Yang[2], Li Gao[2]

[1]*School of Stomatology, Zunyi Medical University, Zunyi 563000, Guizhou, China;* [2]*Department of Periodontal, Stomatological Hospital Affiliated to Zunyi Medical University, Zunyi 563000, Guizhou, China.* [*]*Equal contributors.*

Received December 15, 2024; Accepted October 23, 2025; Epub December 15, 2025; Published December 30, 2025

Abstract: Objectives: Given the lack of effective treatments for periodontal bone tissue regeneration, this study aimed to evaluate the efficacy of Polycaprolactone-Polyethylene glycol (PCL-PEG) electrospun nanofibers combined with amniotic homogenate supernatant (AMH) on periodontal bone repair. Methods: PCL-PEG electrospun nanofibers were prepared by electrospinning and characterized. In vitro, hPDLSCs were divided into control, AMH, PCL-PEG, and PCL-PEG+AMH groups, and real-time polymerase chain reaction (PCR) and western blot assays were used to detect osteogenic genes and proteins (Alkaline Phosphatase (ALP), Collagen Type 1 (COL1), Runt-Related Transcription Factor 2 (RUNX2)) to evaluate cell proliferation and osteogenic differentiation. In vivo, a rat periodontal bone defect model was established. The rats were divided into three groups: a blank control group, a PCL-PEG + PDLSCs group, and a PCL-PEG+AMH + PDLSCs group, and hematoxylin and eosin (HE) staining and micro-computed tomography (Micro-CT) analyzed new bone formation after 4 weeks. Results: PCL-PEG nanofibers had a "fishnet" 3D structure, good hydrophilicity, mechanical strength, and biocompatibility. Both in vitro and in vivo, the PCL-PEG+AMH group exhibited the strongest osteogenic potential and the highest amount of new bone formation. Conclusions: The combination of electrospun nanofibers and AMH can boost periodontal stem cell functions, enhancing alveolar bone repair and providing a new type of support for periodontal bone tissue regeneration.

Keywords: PCL-PEG electrospun nanofibers, amniotic homogenate supernatant, periodontal membrane stem cells, periodontal bone defect, periodontal tissue regeneration

Introduction

The periodontium, composed of the gingiva, alveolar bone, periodontal ligament, and cementum [1], functions to support, attach, and nourish teeth. Among these, alveolar bone plays an important role in the stabilization of teeth and tooth function. When the alveolar bone is damaged, it often causes tooth loosening, and even tooth loss in severe cases, resulting in serious adverse effects on chewing function [2, 3]. Therefore, healthy alveolar bone is particularly important for the stability and function of teeth. In recent years, Tissue engineering has shown great advantages in bone tissue regeneration, and its principle is to combine cells, natural or artificial scaffold materials, and growth factors to support natural tissue regeneration and achieve reconstruction or repair of damaged tissues [4].

Periodontal Ligament stem cells (PDLSCs) are self-renewing, and pluripotent mesenchymal stem cells which are extracted from periodontal tissue, are capable of differentiating into osteoblasts, adipocytes, and chondrocytes [5]. Periodontal stem cells are considered to have the greatest differentiation potential [6]. Studies have reported that PDLSCs used as seed cells to repair defective periodontal bone tissue have achieved ideal results and promoted the regeneration of periodontal bone tissue [7, 8]. The early concept of electrospinning was developed by Anton Formhals in the 1930s [9]. The specific working principle is to apply voltage between a needle and a collecting plate and stretch the droplets of the polymer to form a Taylor cone under the action of the electric force field. When the electric force field is greater than the surface tension of the polymer solution or melt, the charged jet of the polymer

https://doi.org/10.62347/PXMW3056

solution will be ejected, and finally collected on the receiving device to form a fiber film with the random or directional arrangement of fibers [10, 11]. Electrospun nanofibers can be customized according to specific requirements; they have low cost, can simulate the extracellular matrix, promote cell proliferation and differentiation, have good mechanical properties, biocompatibility, anti-degradation ability, and other advantages, and they have been widely used as scaffolds in bone, cartilage, skin and other types of tissue engineering [12-14]. Among them, the synthetic polymer Polycaprolactone (PCL) has good biocompatibility, mechanical strength, and degradation performance, and can better simulate the extracellular matrix, etc., and has been used as a raw material for electrospinning in the field of tissue regeneration [15, 16]. However, due to the lack of cell affinity sites on the surface of PCL, its hydrophilicity is poor and it is a hydrophobic material [17], which is not conducive to cell adhesion and limits its application as an electrospinning material. Among them, the synthetic polymer polyethylene glycol (PEG), which contains abundant ethoxy groups capable of forming hydrogen bonds with water, can be blended with various materials to enhance their hydrophilicity for electrospinning [18]. While an ideal scaffold provides structural support and favorable physical cues, successful periodontal regeneration also relies on a bioactive microenvironment that can stimulate cellular responses and guide tissue formation. To this end, bioactive factors derived from natural sources have garnered significant interest. The human amniotic membrane is a natural polymer composite made of membrane biomaterial, located in the inner layer of the placental membrane, consisting of a single layer of epithelial cells, a basement membrane, and a stroma layer. It is rich in hyaluronic acid, different types of collagen (such as type I, type III, type IV, type V), elastin, laminin, proteoglycan, fibronectin, etc. [19, 20]. Amniotic membrane homogenate (AMH) supernatant is a transparent and stable liquid homogenate supernatant obtained by homogenizing the amniotic membrane and centrifuging. It is widely used in tissue engineering due to its characteristics of convenient collection, low immunogenicity, rich collagen matrix and multiple growth factors, and anti-inflammatory effect [21-23]. We therefore hypothesized that a combination of PCL-PEG electrospun nanofibers and AMH supernatant would create a synergistic system, wherein the nanofibers provide a stable, biomimetic scaffold for cell adhesion and proliferation, and the bioactive constituents in AMH enhance the osteogenic differentiation of PDLSCs.

In this study, PCL-PEG electrospun nanofibers combined with amniotic homogenate supernatant were used to explore the osteogenic differentiation potential of hPDLSCs and the potential feasibility of repairing periodontal bone defects through in vivo and in vitro experiments, providing a certain experimental basis and theoretical basis for using PCL-PEG electrospun nanofibers combined with amniotic homogenate supernatant to repair periodontal bone defects.

Materials and methods

Culture, identification and differentiation potential of human periodontal ligament stem cells (hPDLSCs) for osteogenic, chondrogenic and lipogenic cells.

Isolation, culture, and cloning of hPDLSCs

Human impacted teeth and premolars scheduled for extraction were selected according to the following criteria: ① Aged 18-30 years old, healthy, without systemic diseases; ② The tooth body was extracted intact and without periodontal inflammation.

The periodontal ligament tissue from the root surface was minced and cultured in a bottle containing Dulbecco's Modified Eagle Medium (DMEM) supplemented with 10% fetal bovine serum (FBS) at 37°C, in a 5% CO_2 incubator. When the primary cells were fully covered 80%-85% of the bottom plate, 0.25% trypsin was used for digestion for 2 min and cells were centrifuged for 5 min (800 rpm/min). Cell density was adjusted to 5 to 10 cells/μl using the limiting dilution method. A total of 100 ul cell suspension was inoculated on 96-well plates, and the cells were spread to the bottom plate 1/2 to 2/3, centrifuged for 5 min (800 rpm/min), and then cultured on 6-well plates for further passage. All subsequent experiments were performed using hPDLSCs at passages 3-6. This research was approved by the Ethics Committee of the hospital and informed consent of the patient.

Table 1. Sequence of gene primers

Gene	Sequences
ALP F	CATGAAGGAAAAGCCAAGCAG
ALP R	GGGGCCAGACCAAAGATAGAG
COL1 F	AAAGATGGACTCAACGGTCTC
COL1 R	CATCGTGAGCCTTCTCTTGAG
RUNX2 F	TGGTTACTGTCATGGCGGGTA
RUNX2 R	TCTCAGATCGTTGAACCTTGCTA
GAPDH F	CAGGAGGCATTGCTGATGAT
GAPDH R	GAAGGCTGGGGCTCATTT

Identification of hPDLSCs by flow cytometry

The third generation hPDLSCs at passage 3 were harvested using 0.25% trypsin for 2 minutes, centrifuged for 5 min (800 rpm/min), cleaned and precipitated with phosphate buffered saline (PBS), and then centrifuged again to adjust the concentration to 2×10^6/ml. One rat monoclonal antibody (CD90, CD73, CD44, CD105) as well as the negative control mixture CD19/CD34/CD11b/CD45/HLADR were mixed in a centrifugal tube, vortexed, avoiding light conditions, incubation for 30 min, rinsed, centrifuged for 6 min (1000 rpm/min), with the supernatant discarded, centrifuged again, and PBS added to the resuspension machine for detection.

Assessment of osteogenic, chondrogenic, and adipogenic differentiation potential

The third-generation hPDLSCs were taken, the cell density was adjusted to 1×10^5/ml, and 1 ml was inoculated into the 24-well plate. When the cells were fully covered with 80%-85% of the bottom of the plate, the cells were cleaned with PBS, and the osteogenic, chondrogenic, and lipogenic induction culture medium were added respectively. After continuous induction for 21 days, the corresponding staining solution was added respectively and then observed and photographed under the microscope.

Fabrication and characterization of PCL-PEG electrospun nanofibers

Preparation of PCL-PEG nanofibers: At room temperature, 0.9 g PCL particles and 0.1 g PEG sheets were weighed and added to 8 ml organic solvent (alcohol: hexafluoroisopropyl alcohol = 1:4). The solvent was placed on a magnetic stirrer and stirred for 16 h until it was uniformly clarified. All of them were sucked into a 10 ml syringe and fixed on an electrospinning machine. The receiving distance was set to 20 cm, the voltage was 7 kV, and the propulsion speed was 0.8 ml/h. All electrospinning experiments were carried out at 25°C and relative humidity of 55% for a period of time until the spinning solution was completely spun, and PCL-PEG electrospun nanofibers were collected with aluminum foil. It was dried in an oven at 37°C for 48 hours and stored for later use.

Morphological, hydrophilic, and mechanical characterization

The microstructure of PCL-PEG electrospun nanofibers was observed by scanning electron microscopy after gold spraying on the surface.

Detection of hydrophilicity and stress-strain curve of PCL-PEG electrospun nanofibers: Hydrophilic test: Cut PCL-PEG to the size of 2 cm × 2 cm, take 3 samples for measurement, drop deionized water on the fiber film, and measure the Angle value with the contact Angle measuring instrument.

Stress-strain curve detection: PCL-PEG electrospun nanofibers were cut to 30.0 mm × 20.0 mm and fixed on a universal mechanical measuring instrument. The tensile force was set at 50 N and the tensile speed was set at 1 mm/min to stretch the fiber film until it broke.

Biocompatibility evaluation of PCL-PEG nanofibers

Cell viability assay (CCK-8): The third-generation hPDLSCs were selected and set in a control group and PCL-PEG group, with 5 reports in each group, and the cell concentration was adjusted to 2×10^4 cells/ml. The cells were inoculated with 200 ul in a 48-well plate, and cultured at 37°C in a 5% CO_2 incubator. Both groups were tested every 24 hours: Remove the 24-well plate, rinse with PBS, add 20 ul CCK-8 liquid and 180 ul complete culture medium, and incubate in a constant temperature incubator for 2 hours away from light. Absorb 100 ul liquid from each well and transfer it into the 96-well plate, measure its OD value at 450 nm, and measure it in the same way for 7 days.

Live/dead staining and DAPI staining

The third-generation hPDLSCs were inoculated with 200 ul in 2×10^4/ml into a 48-well plate

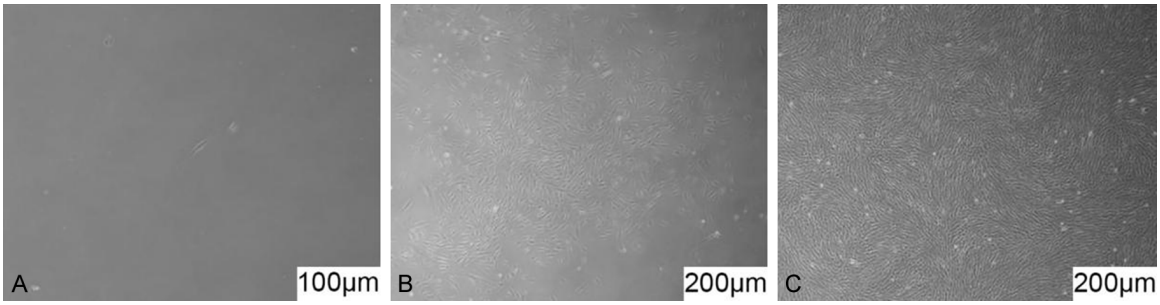

Figure 1. Purification of hPDLSCs by limited dilution (A: 100×; B: 40×; C: 40×). Note: (A) Single human periodontal stem cell; (B) hPDLSCs cloned into clusters 4-5 days later; (C) The first generation of periodontal stem cells.

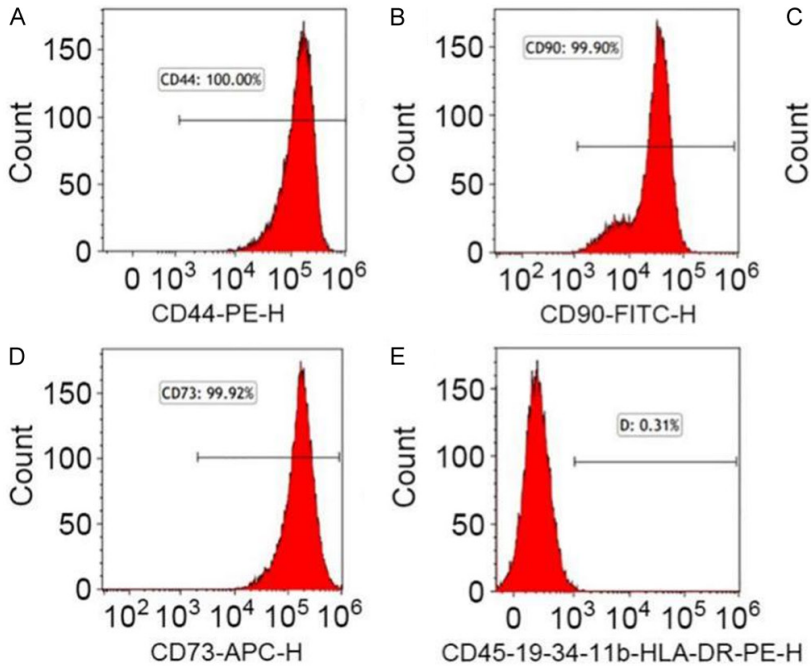

Figure 2. Identification of periodontal stem cells by flow cytometry. Note: A: CD44 positive rate; B: CD90 positive rate; C: CD105 positive rate; D: CD73 positive rate; E: Negative markers (CD45/CD19/CD34/CD11b/HLA-DR) expression.

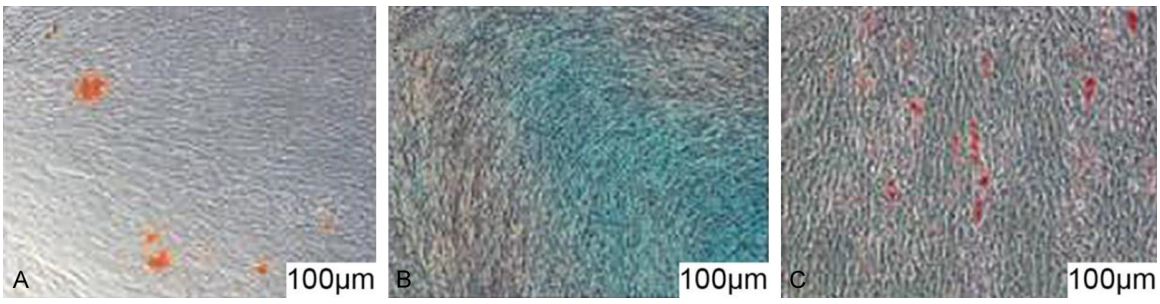

Figure 3. Three-line differentiation of acellular supramniotic periodontal stem cells. Note: A: Alizarin red staining (100×); B: Alcian blue dyeing (100×); C: Oil Red O dyeing (200×).

lined with PCL-PEG electrospun nanofibers and incubated in a constant temperature incubator. The culture plates were taken out on the 2nd and 5th day, washed with PBS, and 100 ul calcein - propyl iodides dye solution was added to each well and placed in a constant temperature incubator for 30 minutes. The solution was discarded, washed with PBS, immediately observed under an inverted fluorescence microscope, and photographed.

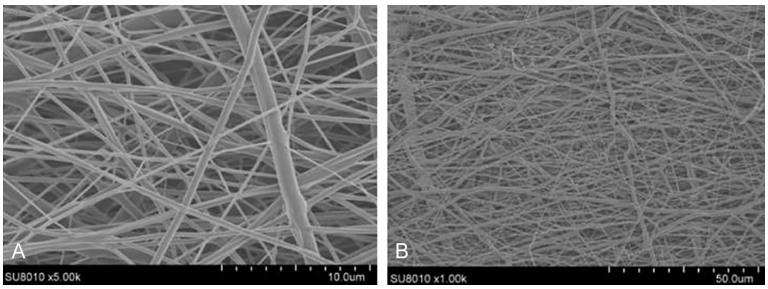

Figure 4. Surface structure of PCL-PEG electrospun nanofibers. Note: A: Fiber structure at 10 μm scale; B: Fiber structure at 50 μm scale.

The third-generation hPDLSCs were taken, counted, and inoculated with 200 ul at 2 × 10^4/ml into 48-well plates lined with PCL-PEG electrospun nanofibers, and incubated in a constant temperature incubator. The culture plates were removed on the 2nd and 5th day, washed with PBS, fixed with 4% paraformaldehyde for half an hour, washed with PBS, and then washed with PBS. An appropriate amount of DAPI staining solution was added to avoid light for 10 minutes, washed with PBS, and immediately placed under an inverted fluorescence microscope for observation and photography.

SEM observation of hPDLSCs growth on fibrous membranes

The third-generation hPDLSCs were taken, counted, and inoculated in a volume of 200 ul at 2 × 10^4/ml into 48-well plates covered with PCL-PEG electrospun nanofibers, and incubated in a constant temperature incubator. The culture plates were removed on the third day, washed with PBS, and the PCL-PEG nanofibers were transferred into glutaraldehyde solution and fixed at room temperature for 2 h. After PBS cleaning, gradient dehydration with ethanol, freeze-drying, and PCL-PEG electrospun nanofibers were glued to the adhesive base, treated with vacuum gold spray, and observed under a scanning electron microscope.

Preparation of amniotic membrane homogenate (AMH) supernatant

The human amniotic membrane was taken from the obstetrics department of the Affiliated Hospital of Zunyi Medical University. The study was reviewed by the Medical Ethics Committee of the Affiliated Stomatology Hospital of Zunyi Medical University, and the maternal informed consent was in line with relevant ethical requirements. The maternal age was 20-35 years old, healthy and free of systemic and infectious diseases. The amniotic surface of the placenta was repeatedly rinsed with sterile PBS, peeled and cut, and PBS was added (ratio 1:1). After homogenization at low temperature, PBS was added (ratio 1:4). The supernatant was centrifuged at 4°C, 2000 rpm, 10 min, and then stored in the freezer at -80°C for later use.

In vitro osteogenic differentiation assays

Experimental groups: ① Control group (Osteogenic induction medium group): osteogenic induction medium group (OS group); ② Experimental group: AMH group (amniotic homogenate supernatant + osteogenic induction medium group); PCL-PEG group (PCL-PEG electrospun nanofibers + osteogenic induction medium group); PCL-PEG+AMH group (PCL-PEG electrospun nanofibers combined with amniotic homogenate supernatant + osteogenic induction medium group).

Alkaline phosphatase (ALP) activity and staining (BCIP/NBT)

BCIP/NBT staining: The third-generation hPDLSCs were taken, the cell concentration was adjusted to 1.0 × 10^5/ml, and 1 ml was inoculated into a 12-well plate for culture. When the cells covered 80% of the bottom of the pores, the cells were rinsed with PBS, and the osteogenic induction solution was added to the OS group and the experimental group respectively. After continuous induction for 7 days, cells were rinsed with PBS and treated with 4% paraformaldehyde for 30 min. Rinse with PBS, add BCIP/NBT staining solution under dark, stain for 30 min, rinse with PBS, and observe under the microscope.

ALP: The third-generation hPDLSCs were taken, the cell concentration was adjusted to 1.0 × 10^5/ml, and 1 ml was inoculated on 12-well plates. When the cells fully covered 80% of the bottom of the pores, the osteogenic induction solution was added to the OS group and the experimental group, respectively, for

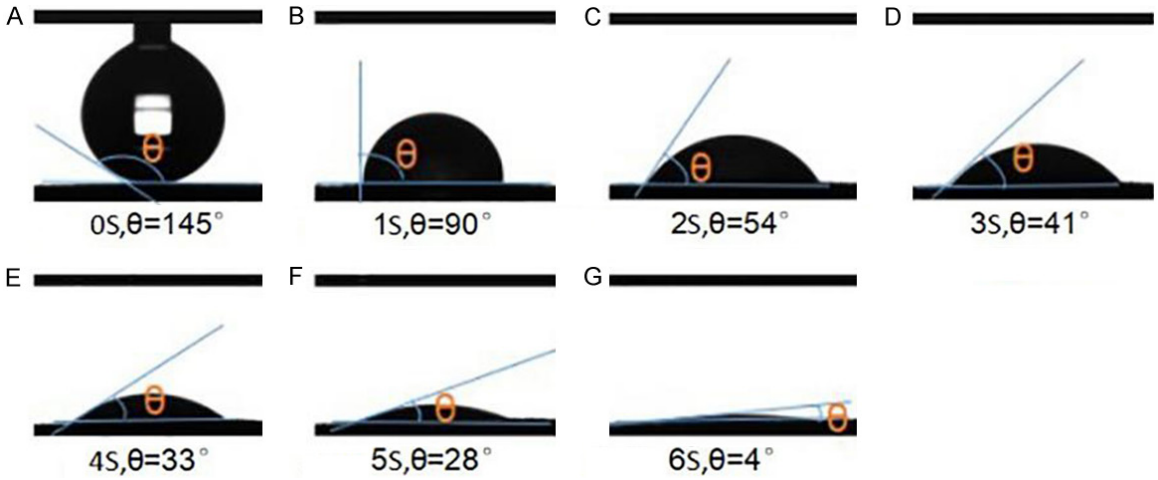

Figure 5. Hydrophilicity detection of PCL-PEG electrospun nanofibers. Note: A: Contact angle at 0 s; B: Contact angle at 1 s; C: Contact angle at 2 s; D: Contact angle at 3 s; E: Contact angle at 4 s; F: Contact angle at 5 s; G: Contact angle at 6 s.

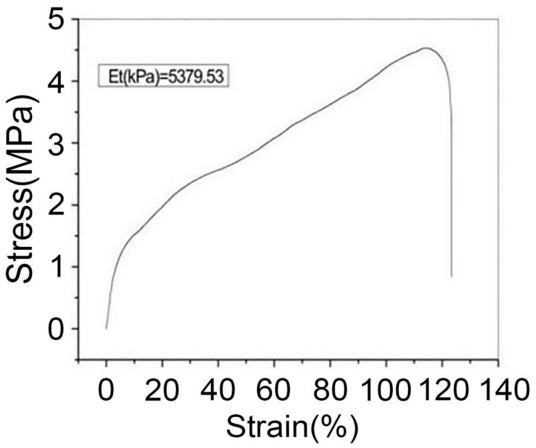

Figure 6. Stress-strain measurement of PCL-PEG electrospun nanofibers.

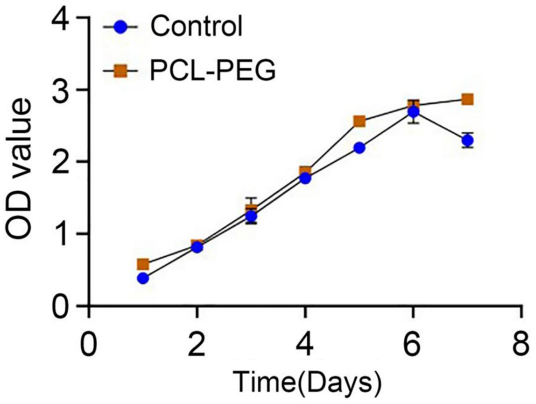

Figure 7. The proliferation of periodontal stem cells in the two groups was detected by Cell Counting Kit-8 (CCK-8) method.

continuous induction for 7 days, the osteogenic induction solution was added to PBS, and 100 μl 1% triton X was added. The protein concentration of each group was determined by the BCA method. The ALP activity of each group = (measured optical density (OD) value - blank OD value)/(standard OD value - blank OD value) × phenol standard concentration ÷ protein concentration of the sample to be measured.

Mineralization nodule detection (alizarin red S staining)

The third-generation hPDLSCs were taken, and 1 ml was inoculated into a 12-well plate at a cell concentration of 1.0 × 10^5/ml. When the cells covered 80% of the bottom of the pores, they were rinsed with PBS. The osteogenic induction solution was added to the OS group and the experimental group, respectively, and continuously induced for 21 d, rinsed with PBS, treated with 4% paraformaldehyde for 30 min, and rinsed with PBS. A total of 0.5 ml alizarin red S dye solution was added to each well, stained away from light for 30 minutes, rinsed with double steaming water, and observed under a microscope.

Gene expression analysis by real-time quantitative PCR (RT-qPCR)

The third-generation hPDLSCs were taken, the cell concentration was adjusted to 1.0 × 10^5/ml, and 2 ml were inoculated into the 6-well

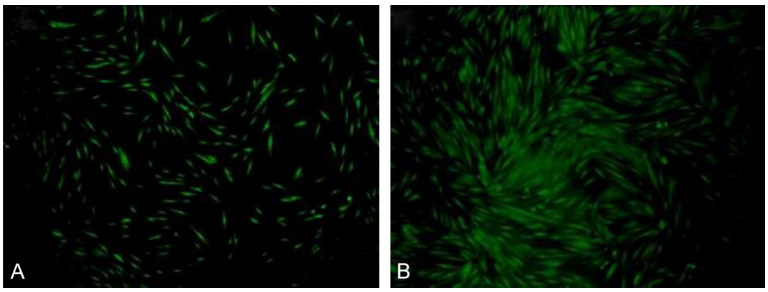

Figure 8. Cell viability and distribution on PCL-PEG nanofibers detected by Calcein-AM/Propidium Iodide (PI) staining (scale: 200 μm). Note: A: Fluorescence image after 2 days of culture. Living cells are stained green (Calcein-AM); B: Fluorescence image after 5 days of culture. The number of living cells (green) significantly increased, indicating good biocompatibility and support for cell proliferation. (Note: Red staining for dead cells was rarely observed, not shown here).

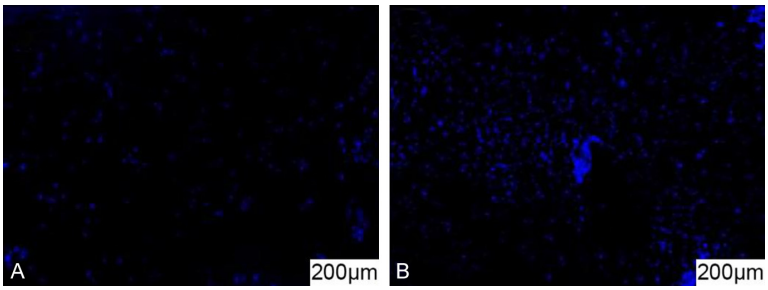

Figure 9. DAPI staining (scale: 200 μm). Note: A: DAPI staining image after 2 days of culture; B: DAPI staining image after 5 days of culture. The significant increase in cell nuclei (blue) confirms the active proliferation of hPDLSCs on the scaffold.

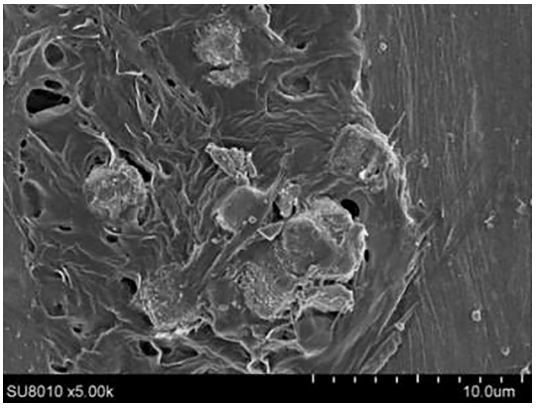

Figure 10. Sem results (scale: 10 μm).

plate. When the cells reached 80% confluence, they were washed with PBS, and the osteogenic induction solution was added to the OS group and the experimental group, respectively. After continuous induction for 7 days, the total cell RNA was extracted using NAISo-PLUS according to the instructions. complementary DNA (cDNA) was synthesized by reverse transcription using PrimeScript®RT kit. The expression of osteogenic genes Alkaline Phosphatase (ALP), Collagen Type 1 (COL1), and Runt-Related Transcription Factor 2 (RUNX2) was detected by the ABI Prism7300 system in RT-PCR reaction by SYBR®Premix Ex TaqTM (Perfect Real Time). PCR was performed as follows: 1 cycle at 95°C for 30 seconds, then 40 cycles at 95°C for 10 seconds, 40 seconds at 60°C, then 5 seconds at 65°C, 30 seconds at 60°C, and 5 seconds at 95°C. The primer sequence is shown in **Table 1**. We did the quantification independently, in triplicate.

Protein expression analysis by western blot

The third-generation hPDLSCs were taken, the cell concentration was adjusted to 1.0 × 10^5/ml, and 2 ml were inoculated into the 6-well plate. When the cells covered 80% of the bottom of the well, the cells were rinsed with PBS. The osteogenic induction solution was added to the OS group and the experimental group, and the cells were continuously induced for 7 days and then rinsed with PBS. The mixture of RIPA + phenylmethylsulfonyl fluoride (PMSF) + protein phosphatase inhibitor (100:1:1) was added, and centrifuged at low temperature and high speed for 5 min, the supernatant was absorbed, the protein concentration was determined by BCA method, the transfer membrane was separated by gel electrophoresis, and sealed with skim milk for 2 h. The primary antibody working medium was added, washed with TBST 18 h later, and incubated in the secondary antibody chamber for 40 minutes. The Western HRP luminescent substrate was exposed, and the expression of ALP, COL1, and RUNX2 osteoblast protein was detected by Image J.

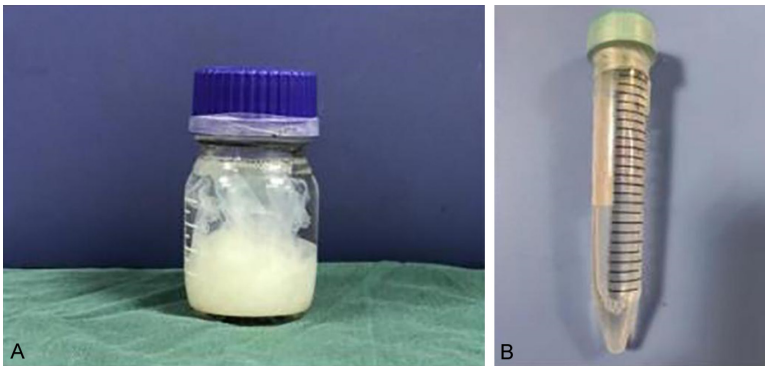

Figure 11. Amniotic membrane and amniotic homogenate supernatant (AMH). Note: A: A fresh human amniotic membrane, appearing as a white or light yellow translucent membrane; B: The final product after homogenization and centrifugation: the transparent and clear AMH.

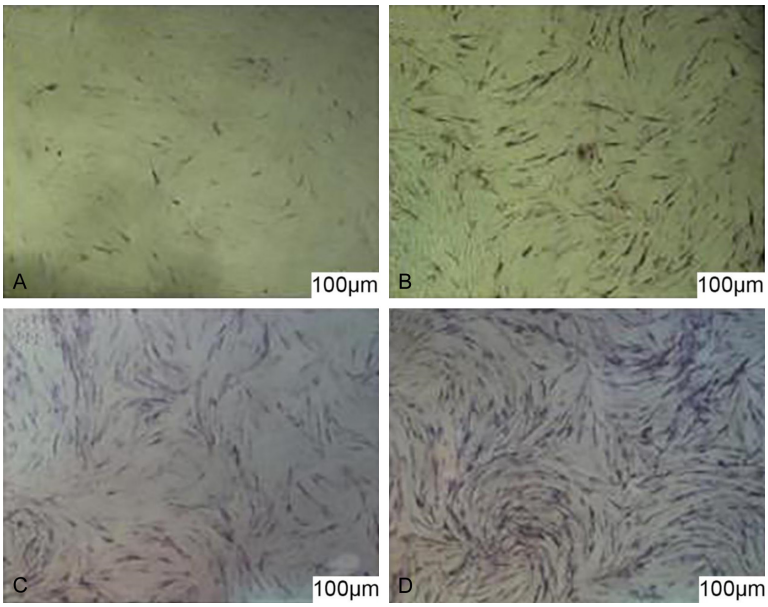

Figure 12. BCIP/NBT staining (A: Osteogenic induction medium (OS) group; B: AMH group; C: PCL-PEG group; D: PCL-PEG+AMH group).

In vivo repair of periodontal bone defects in a rat model

Eighteen SD rats were randomly divided into three groups. After weighing and anesthesia, a defect model of 3 mm × 2 mm × 1 mm (length 3 mm, width 2 mm, depth 1 mm) was established in the distal alveolar bone of mandibular incisor teeth. Group A was the control group. Group B was a 7-day osteogenic induction complex co-cultured with PCL-PEG electrospun nanofibers and periodontal stem cells, group C was a 7-day osteogenic induction complex co-cultured with amniotic homogenate supernatant and periodontal stem cells. Four weeks later, the mandible was removed, fixed with 4% paraformaldehyde, and the mandible was scanned by Micro-CT. The formic acid decalcification solution was treated for a week, followed by dehydration, pruning, embedding, slicing, dyeing, sealing, and other steps, and finally microscopic examination.

Statistical analysis

All data were analyzed and processed by SPSS 29.0 statistical software, and all data were expressed as mean ± standard deviation. An Independent sample t-test was used for the two comparisons, and a one-way analysis of variance was used for intergroup comparison. A = 0.05 was used as the test level, and $P < 0.05$ indicated that the difference was statistically significant.

Results

Growth characteristics, identification of periodontal stem cells

Single periodontal cells were screened by a limited dilution method and cloned and purified for culture (**Figure 1A**). After 4-5 days of culture, the cells gathered into clusters (**Figure 1B**). The cells adhering to the wall in the pore plate grew rapidly and grew in a spiral shape. Most cells were long spindle-shaped or polygon, and the cytoplasm was full (**Figure 1C**).

Flow cytometric analysis showed that hPDLSCs were highly positive for mesenchymal stem cell markers CD44 (100%), CD90 (99.90%), CD73 (99.92%), and CD105 (95.07%), but negative for hematopoietic lineage markers CD45, CD11b, CD19, CD34, and HLA-DR (0.31%). CD105, CD90, high CD73, CD44 expression, CD45/CD11b/CD19/CD34/low HLA-DR expression (**Figure 2A-E**), between hPDLSCs con-

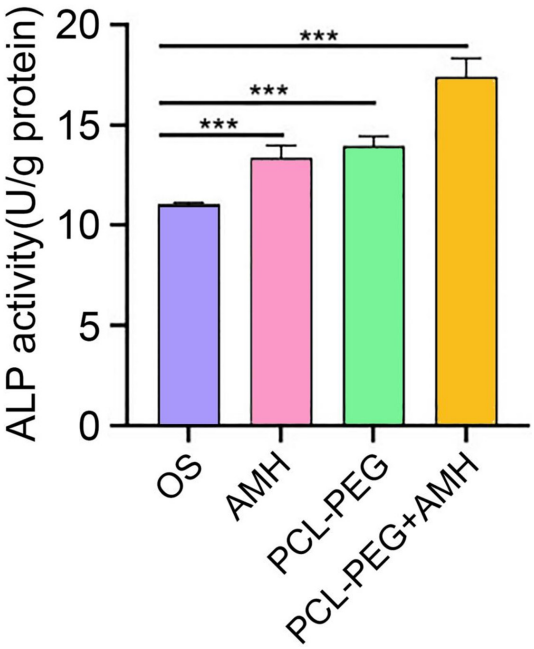

Figure 13. ALP activity test (***indicates P < 0.05).

form to the definition of mesenchymal stem cells.

Differentiation ability of periodontal stem cells after 21 days of induction by osteogenic, chondrogenic, and lipogenic induction solution

The periodontal stem cells were stained with alizarin red, Alcian blue, and oil red O respectively, and the results showed irregular red calcified nodules with alizarin red staining (**Figure 3A**). Alcian blue staining (**Figure 3B**) showed large patches of blue chondroid cells. Oil red O staining (**Figure 3C**) shows a large number of deeply stained red fat droplets.

Properties of PCL-PEG electrospun nanofibers

Under scanning electron microscopy, PCL-PEG electrospun nanofibers showed a three-dimensional "fishing network" structure, and the fiber diameter and pore size were different (**Figure 4**). PCL-PEG electrospun nanofibers have good hydrophilicity, and the θ Angle is close to 0° in about 6 seconds, which is close to complete hydrophilicity (**Figure 5A-G**). The mechanical properties were evaluated, showing the PCL-PEG electrospun nanofibers were stretched to about 1.2 times the original length, a complete fracture occurred with a maximum strength of about 4.5 MPa (**Figure 6**).

Biocompatibility detection of PCL-PEG electrospun nanofibers

The results of the Cell Counting Kit-8 (CCK-8) method showed (**Figure 7**) that periodontal stem cells in the control group and the PCL-PEG group proliferated rapidly in the first 6 days, with the trend being roughly the same, but the cell proliferation rate in the PCL-PEG group was higher than that in control group, and the cell proliferation rate in PCL-PEG group reached a plateau after 6 days, while the cell proliferation rate slowed down. However, after 6 days in the control group, because the cells at the bottom of the pore plate were completely overgrown, there was no space for cell growth, the proliferation of cells was significantly inhibited, and some cells died. Calcein-AM/PI staining revealed a high density of viable cells (green) on the PCL-PEG nanofibers on both days 2 and 5, with minimal detection of dead cells (red) (**Figure 8**). Concurrently, DAPI staining confirmed a significant increase in total cell number from day 2 to day 5 (**Figure 9**), indicating active proliferation. Scanning electron microscope results (**Figure 10**) showed that after the PCL-PEG electrospun nanofibers were dehydrated by an ethanol gradient, some fibers of the fiber membrane dissolved, and the microstructure changed from an irregular network structure to porous structure. The growth of periodontal stem cells embedded in the space was observed.

Preparation of supernatant of amniotic membrane homogenate

A fresh amniotic membrane is a white or light yellow translucent membrane (**Figure 11A**), and the supernatant of the amniotic homogenate is transparent and clear liquid (**Figure 11B**).

Influence of each group on osteogenic differentiation of periodontal stem cells

5-Bromo-4-chloro-3-indolyl phosphate/Nitro blue tetrazolium (BCIP/NBT) staining results in the PCL-PEG+AMH group had the deepest coloring depth and the widest coloring area, followed by PCL-PEG group and AMH group, and OS group had shallowest coloring depth and smallest coloring area (**Figure 12**).

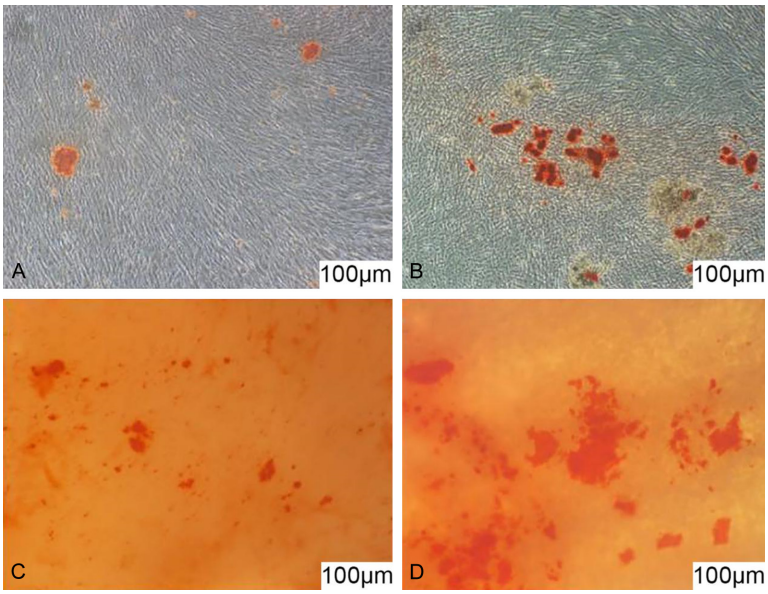

Figure 14. Coloring of alizarin red. A: OS group; B: AMH group; C: PCL-PEG group; D: PCL-PEG+AMH group.

ALP activity test results in quantitative values in the AMH group, PCL-PEG group, and PCL-PEG+AMH group were higher than those in the OS group, and the difference was statistically significant ($P < 0.05$), among which PCL-PEG+AMH had the best bone composition ability (**Figure 13**).

Alizarin red staining was used to detect the mineralized nodules: PCL-PEG+AMH group had the reddest calcified nodules, followed by PCL-PEG group and AMH group, and OS group had the least red calcified nodules (**Figure 14**).

mRNA expression levels related to osteogenesis were detected by RT-PCR: The expressions of osteogenic genes ALP (**Figure 15A**), COL1 (**Figure 15B**), and RUNX2 (**Figure 15C**) were up-regulated, and up-regulation was highest in PCL-PEG+AMH group, which was higher than that in OS group, with a statistical significance ($P < 0.05$).

Western blot was used to detect the expression of osteoblast-related proteins: Compared with the OS group, the expression levels of osteoblast-related proteins ALP (**Figure 16A**), COL1 (**Figure 16B**), and RUNX2 (**Figure 16C**) increased, and the expression levels of the PCL-PEG+AMH group were the highest, which was also confirmed by quantified gray values (**Figure 17**) ($P < 0.05$).

PCL-PEG electrospun nanofibers combined with amniotic homogenate supernatant to repair periodontal bone defects in rats

The biocompatibility test results of PCL-PEG electrospun nanofibers showed that there was no obvious inflammatory cell infiltration and no significant difference among the three groups (**Figure 18**), indicating that PCL-PEG electrospun nanofibers had no toxicity to the important internal tissues of rats. Therefore it is relatively safe to implant in SD rats.

Periodontal bone defect repair in rats: HE staining showed no new bone tissue in the periodontal bone defect area in group A. Some new bone tissue was found in the periodontal bone defect area of group B. There was more new bone tissue in the periodontal bone defect area in Group C than in Group B, and fibrous tissue hyperplasia was observed in Group B and Group C (**Figure 19**). Micro-CT showed no new bone formation in the periodontal bone defect area in group A. A small amount of new bone tissue was generated in the periodontal bone defect area in group B. A large amount of new bone tissue was generated in the periodontal bone defect area of group C (**Figure 20**).

Discussion

Conventional periodontal therapy, such as scaling and root planing or flap surgery, primarily aims at debridement and infection control. While effective in managing inflammation, these methods often fall short of achieving the ultimate goal of periodontal treatment: the regeneration of lost periodontal tissues and the restoration of their original architecture and function. True regeneration relies on the principles of tissue engineering.

At present, it is believed that periodontal tissue engineering should have at least the following three conditions: 1. Stem cell population with osteogenic, cementoblastic, and periodon-

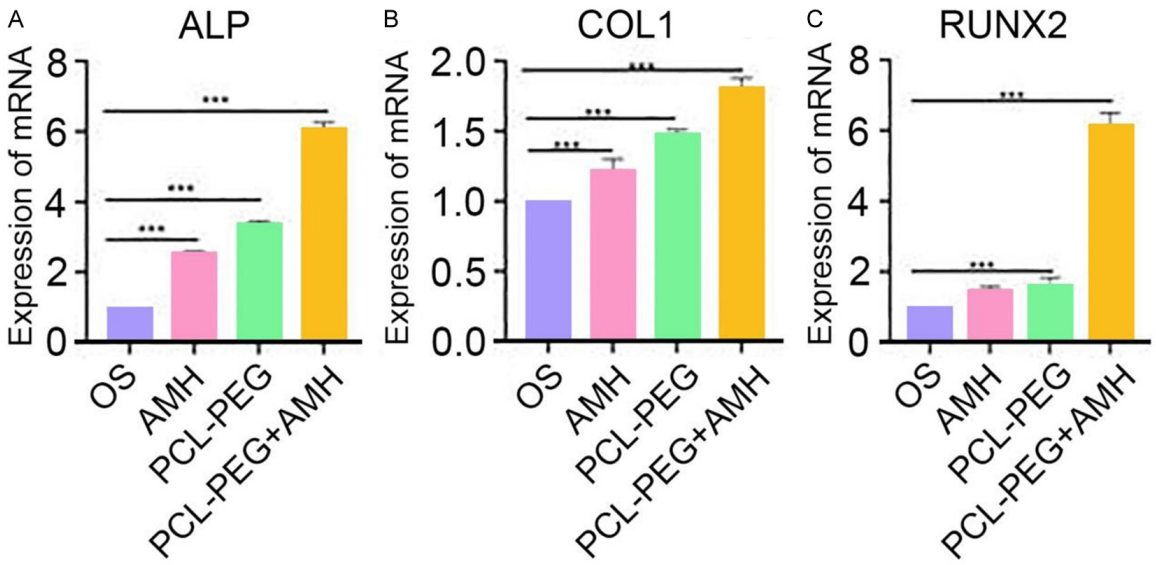

Figure 15. Expression of osteogenic genes (A: ALP; B: COL1; C: RUNX2) detected by RT-PCR (***means P < 0.05).

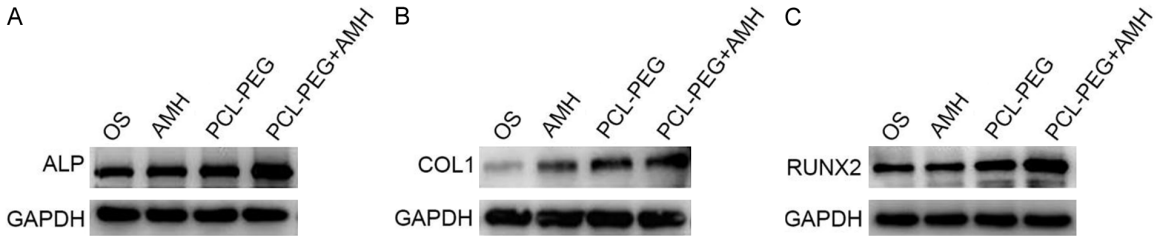

Figure 16. Western Blot analysis of osteoblast-related protein expression (A: ALP; B: COL1; C: RUNX2).

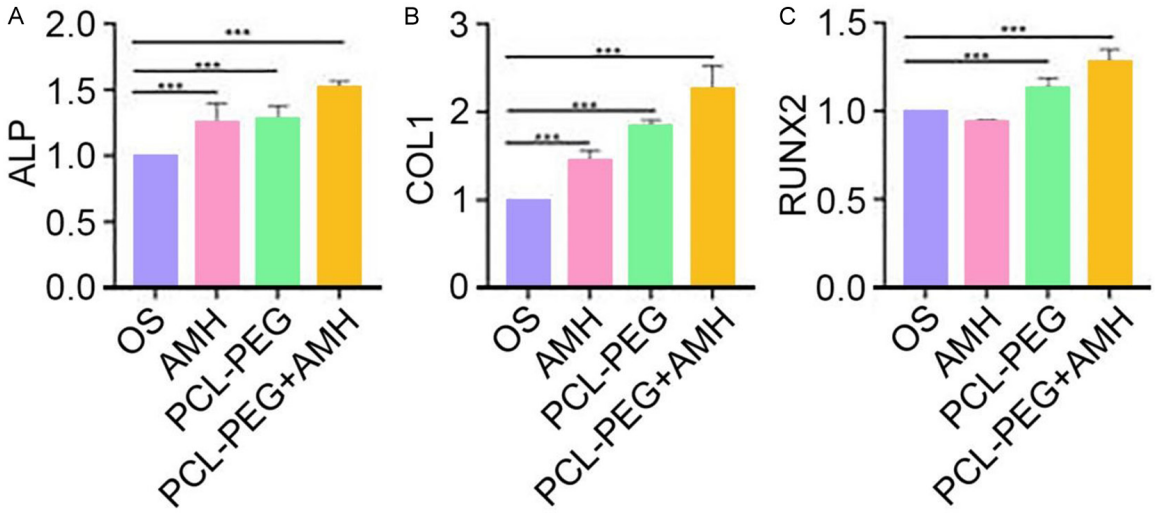

Figure 17. Quantitative analysis of gray value of osteogenic proteins (A: ALP; B: COL1; C: RUNX2) (***indicates P < 0.05).

tal membrane-forming potential; Human periodontal membrane stem cells have strong proliferation and differentiation ability and are the most studied odontogenic mesenchymal stem cells in periodontal tissue engineering [24]. In this experiment, hPDLSCs were obtained by

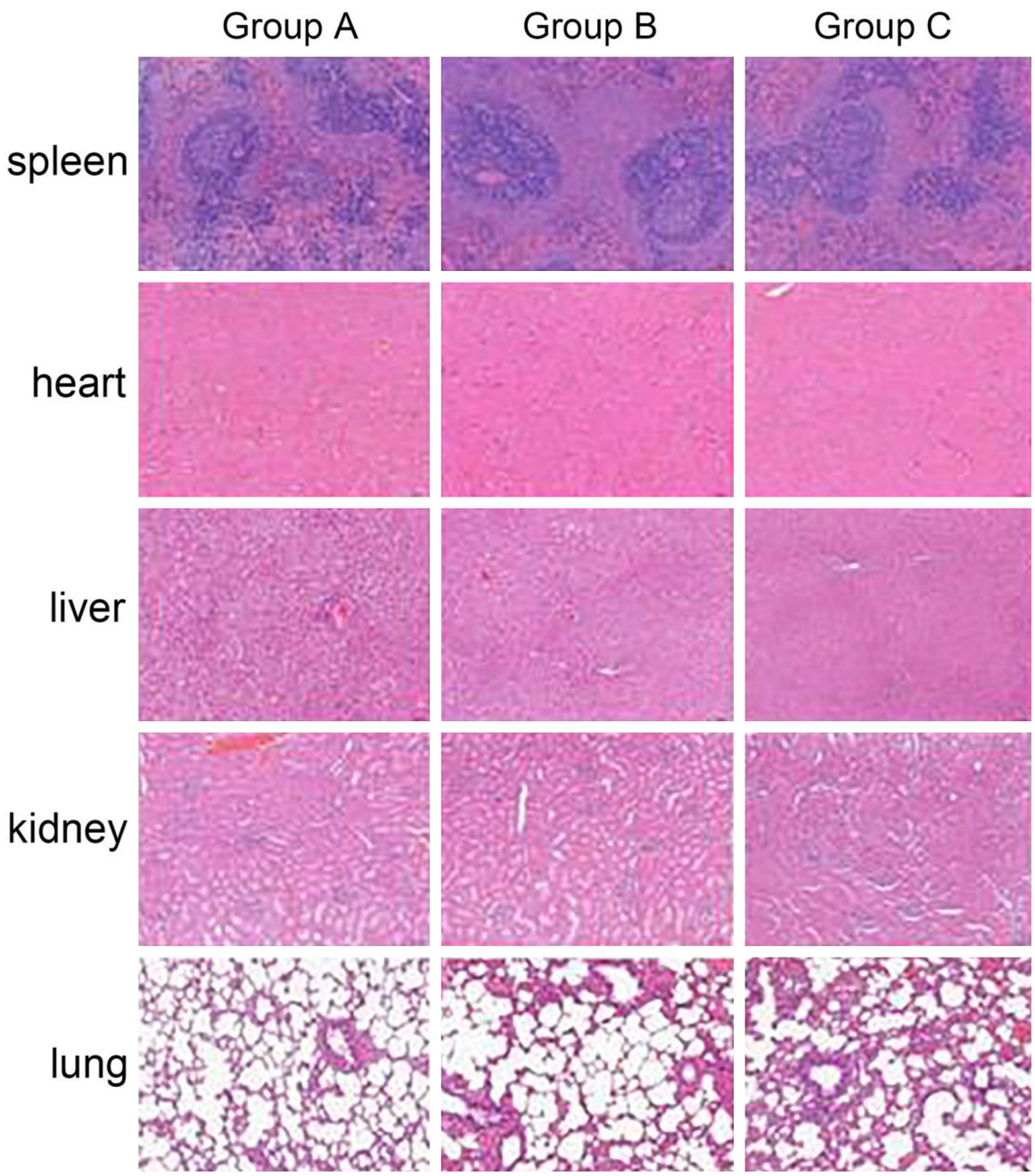

Figure 18. Histological observation of important internal organs in rats (100×).

enzyme digestion and limited dilution cloning, and the cells were long spindle-shaped, and polygon. Flow cytometry was used to identify mesenchymal stem cells. The induction of hPDLSCs by osteogenesis, chondrogenesis, and lipogenesis indicated that HPDLSCs have multidirectional differentiation potential. Second, the support material plays a supporting role; Scaffold materials play important roles in periodontal tissue engineering and should have appropriate mechanical properties, hydrophilicity, layered structure, porosity, etc. [25-27]. The PCL-PEG electrospun nanofibers prepared in this experiment showed a three-dimensional mesh porous structure, and their mechanical properties and hydrophilicity could meet the requirements of periodontal scaffold materials. In this study, after co-culture of hPDLSCs with PCL-PEG electrospun nanofibers, it was found that PCL-PEG electros-

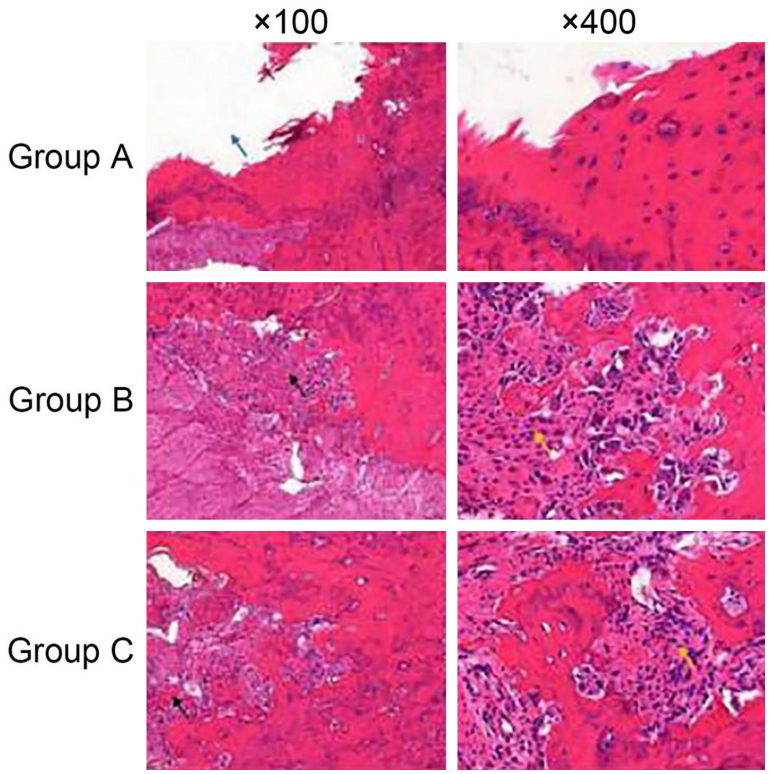

Figure 19. Hematoxylin and eosin (HE) staining (Note: Blue arrow indicates no new bone formation; Black arrows indicate new bone formation; Yellow arrows indicate fibrous tissue hyperplasia).

pun nanofibers had no cytotoxicity, could promote the proliferation of hPDLSCs, and had good biocompatibility. Amniotic homogenate supernatant has the advantages of a simple preparation method, rich in a variety of growth factors and broad-spectrum antibacterial activity [28], and has received extensive attention in tissue engineering, especially in the regeneration treatment of corneal tissue [29, 30]. In this study, PCL-PEG electrospun nanofibers combined with 16 mg/L amniotic homogenate supernatant were co-cultured with periodontal stem cells to explore the effect of PCL-PEG electrospun nanofibers on osteogenic differentiation of periodontal stem cells. By BCIP/NBT staining and ARS staining, it was found that the PCL-PEG+AMH group with BCIP/NBT staining had the deepest staining and the widest area, and the PCL-PEG+AMH group with ARS staining had the most calcium nodules. The 7-day ALP activity in the PCL-PEG+AMH group was the highest, and the difference was statistically significant ($P < 0.05$). RT-PCR and Western blot results showed that: The expression levels of bone-related genes (ALP, COL1, RUNX2) and osteogenic proteins (ALP, COL1, RUNX2) of PCL-PEG+AMH were significantly increased, and were significantly higher than those of OS, AMH, and PCL-PEG groups, with statistical significance ($P < 0.05$). The results indicated that PCL-PEG electrospun nanofibers combined with amniotic homogenate supernatant could synergically promote osteogenic differentiation of periodontal stem cells.

In order to further explore whether the "engineered matrix" composed of PCL-PEG electrospun nanofibers, amniotic homogenate supernatant, and periodontal stem cells can effectively repair the periodontal bone defect in rats, this study implanted the "matrix" into the distal periodontal bone defect in rats' mandibular incisor for 4 weeks, and tested the new bone tissue by HE staining and Micro-CT. Micro-CT is a method that can capture detailed anatomical images of bone and build informative 3D models for structural analysis, with high resolution and sensitivity to detect subtle changes in bone [31, 32]. The results of histology and Micro-CT were similar, suggesting that the newly formed bone tissues in the PCL-PEG electrospun nanofibers combined with amniotic homogenate supernatant and hPDLSCs were significantly better than those in the other two groups. It is suggested that the composite matrix can achieve a good therapeutic effect in repairing the damaged periodontal bone tissue. In addition, the important visceral tissues of the three groups of rats were also detected in this experiment, and the results of tissue slices showed that there were no obvious abnormalities in the visceral tissues, suggesting that the implant was non-toxic and relatively safe. The possible reasons are the good biocompatibility and hydrophilicity of PCL-PEG electrospun nanofibers, which is conducive to cell adhesion and growth, and creates a good environment for survival. The three-dimensional network provides more space for cell growth, which is conducive to cell adhesion and

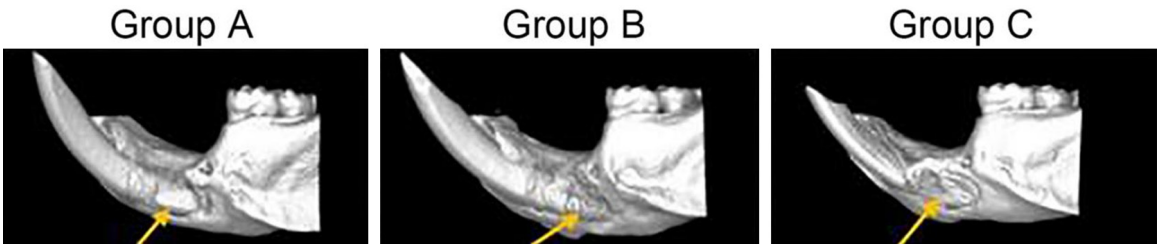

Figure 20. Results of Micro-CT 3D reconstruction of the mandible 4 weeks after surgery (Note: arrows indicate the location of new bone formation).

growth, extracellular matrix precipitation, nutrient and oxygen entry, and metabolite elimination. Good mechanical properties for the new periodontal bone tissue help provide support. Meanwhile, the supernatant of the amniotic homogenate is rich in a variety of cell growth factors, such as basic fibroblast growth factors, which play a variety of biological roles in regeneration and repair of tissue damage; insulin-like growth factor can promote cell migration, proliferation, and differentiation, induce collagen and matrix synthesis, and participate in alveolar bone formation; transforming growth faction-β can induce DNA and fibrin synthesis and regulation osteogenic differentiation [33-35]. Moreover, the amniotic homogenate supernatant contains a variety of collagen proteins (such as type I, type III, type IV, and type V), which may also be beneficial to periodontal bone tissue regeneration. Although the composite matrix shows a certain prospective value in the regeneration of periodontal bone tissue, how to use the advantages of the two and the specific mechanism of osteogenesis need to be further studied.

Conclusion

In summary, PCL-PEG electrospun nanofibers combined with AMH supernatant synergically enhanced the osteogenic differentiation of hPDLSCs in vitro. After co-culture of PCL-PEG electrospun nanofibers combined with amniotic homogenate supernatant and hPDLSCs, PCL-PEG electrospun nanofibers combined with amniotic homogenate supernatant and HPDLSCS were implanted into periodontal bone defects in animals, it could promote periodontal bone tissue regeneration.

Future outlook

PCL-PEG electrospun nanofibers have attracted extensive attention in the field of tissue engineering due to their excellent mechanical properties, hydrophilicity, and biocompatibility. Amniotic homogenate supernatant has many excellent properties, such as being rich in a variety of growth factors, collagen, etc., which makes the application in the field of tissue regeneration achieve good results. Our results show that the combination of the two can promote the osteogenic differentiation of periodontal stem cells in vitro, and the “engineered matrix” formed in vivo can effectively repair periodontal bone defects in rats. However, there are still many problems to be solved, including how to better combine the two, as well as the specific osteogenic mechanism, which need to be further studied.

Acknowledgements

This work was supported by the National Natural Science Foundation of China (820-60204); Science and Technology Department of Guizhou Province (No. ZK[2021] 437); Science and Technology Fund of Guizhou Provincial Health Commission, (No.gzwkj2023-202), Project leader: Gao Li.

Disclosure of conflict of interest

None.

Address correspondence to: Li Gao, Department of Periodontal, Stomatological Hospital Affiliated to Zunyi Medical University, No. 143 Dalian Road, Huichuan District, Zunyi 563000, Guizhou, China. Tel: +86-0851-28635721; E-mail: lianpan020417-8337@126.com

References

[1] Staples RJ, Ivanovski S and Vaquette C. Fibre guiding scaffolds for periodontal tissue engineering. J Periodontal Res 2020; 55: 331-341.
[2] Hernández-Monjaraz B, Santiago-Osorio E, Monroy-García A, Ledesma-Martínez E and

Mendoza-Núñez V. Mesenchymal stem cells of dental origin for inducing tissue regeneration in periodontitis: a mini-review. Int J Mol Sci 2018; 19: 944.
[3] Sanz M, del Castillo AM, Jepsen S, Gonzalez-Juanatey JR, D'Aiuto F, Bouchard P, Chapple I, Dietrich T, Gotsman I, Graziani F, Herrera D, Loos B, Madianos P, Michel JB, Perel P, Pieske B, Shapira L, Shechter M, Tonetti M, Vlachopoulos C and Wimmer G. Periodontitis and cardiovascular diseases: consensus report. J Clin Periodontol 2020; 47: 268-288.
[4] Borrelli MR, Hu MS, Longaker MT and Lorenz HP. Tissue engineering and regenerative medicine in craniofacial reconstruction and facial aesthetics. J Craniofac Surg 2020; 31: 15-27.
[5] Seo BM, Miura M, Gronthos S, Bartold PM, Batouli S, Brahim J, Young M, Robey PG, Wang CY and Shi S. Investigation of multipotent postnatal stem cells from human periodontal ligament. Lancet 2004; 364: 149-155.
[6] Lee JS, Yi JK, An SY and Heo JS. Increased osteogenic differentiation of periodontal ligament stem cells on polydopamine film occurs via activation of integrin and PI3K signaling pathways. Cell Physiol Biochem 2014; 34: 1824-1834.
[7] Park JY, Jeon SH and Choung PH. Efficacy of periodontal stem cell transplantation in the treatment of advanced periodontitis. Cell Transplant 2011; 20: 271-285.
[8] Shi H, Zong WY, Xu XY and Chen JQ. Improved biphasic calcium phosphate combined with periodontal ligament stem cells may serve as a promising method for periodontal regeneration. Am J Transl Res 2018; 10: 4030-4041.
[9] Hong J, Yeo M, Yang GH and Kim G. Cell-electrospinning and its application for tissue engineering. Int J Mol Sci 2019; 20: 6208.
[10] Chapman BS, Mishra SR and Tracy JB. Direct electrospinning of titania nanofibers with ethanol. Dalton Trans 2019; 48: 12822-12827.
[11] Tan GX, Wang LJ, Pan WS and Chen K. Polysaccharide electrospun nanofibers for wound healing applications. Int J Nanomedicine 2022; 17: 3913-3931.
[12] Li Y, Liu Y, Xun X, Zhang W, Xu Y and Gu D. Three-dimensional porous scaffolds with biomimetic microarchitecture and bioactivity for cartilage tissue engineering. ACS Appl Mater Interfaces 2019; 11: 36359-36370.
[13] Liu W, Bi W, Sun Y, Wang L, Yu X, Cheng R, Yu Y and Cui W. Biomimetic organic-inorganic hybrid hydrogel electrospinning periosteum for accelerating bone regeneration. Mater Sci Eng C Mater Biol Appl 2020; 110: 110670.
[14] Mozaffari A and Parvinzadeh Gashti M. Air plasma functionalization of electrospun nanofibers for skin tissue engineering. Biomedicines 2022; 10: 617.
[15] Murab S, Gruber SMS, Lin CJ and Whitlock P. Elucidation of bio-inspired hydroxyapatie crystallization on oxygen-plasma modified 3D printed poly-caprolactone scaffolds. Mater Sci Eng C Mater Biol Appl 2020; 109: 110529.
[16] Ramírez-Cedillo E, Ortega-Lara W, Rocha-Pizaña MR, Gutierrez-Uribe JA, Elías-Zúñiga A and Rodríguez CA. Electrospun polycaprolactone fibrous membranes containing Ag, TiO_2 and $Na_2Ti_6O_{13}$ particles for potential use in bone regeneration. Membranes (Basel) 2019; 9: 12.
[17] Yousefi P, Dini G, Movahedi B, Vaezifar S and Mehdikhani M. Polycaprolactone/chitosan core/shell nanofibrous mat fabricated by electrospinning process as carrier for rosuvastatin drug. Polym Bull 2022; 79: 1627-1645.
[18] Pan L, Yang J and Xu L. Preparation and characterization of simvastatin-loaded PCL/PEG nanofiber membranes for drug sustained release. Molecules 2022; 27: 7158.
[19] Mohammed YA, Farouk HK, Gbreel MI, Ali AM, Salah AA, Nourelden AZ and Gawad MMA. Human amniotic membrane products for patients with diabetic foot ulcers. do they help? a systematic review and meta-analysis. J Foot Ankle Res 2022; 15: 71.
[20] Su YN, Zhao DY, Li YH, Yu TQ, Sun H, Wu XY, Zhou XQ and Li J. Human amniotic membrane allograft, a novel treatment for chronic diabetic foot ulcers: a systematic review and meta-analysis of randomised controlled trials. Int Wound J 2020; 17: 753-764.
[21] Kubo M, Sonoda Y, Muramatsu R and Usui M. Immunogenicity of human amniotic membrane in experimental xenotransplantation. Invest Ophthalmol Vis Sci 2001; 42: 1539-1546.
[22] Sket T, Ramuta TZ, Erjavec MS and Kreft ME. Different effects of amniotic membrane homogenate on the growth of uropathogenic and infection and drug resistance. Infect Drug Resist 2019; 12: 3365-3375.
[23] Wu MF, Stachon T, Langenbucher A, Seitz B and Szentmáry N. Effect of Amniotic Membrane Suspension (AMS) and Amniotic Membrane Homogenate (AMH) on human corneal epithelial cell viability, migration and proliferation in vitro. Curr Eye Res 2017; 42: 351-357.
[24] Pan J, Deng J, Yu L, Wang Y, Zhang W, Han X, Camargo PHC, Wang J and Liu Y. Investigating the repair of periodontal bone defects by gelatin methacrylate hydrogels-encapsulated human periodontal ligament stem cells. J Mater Sci Mater Med 2020; 31: 3.
[25] Deng Y, Zhang M, Chen X, Pu X, Liao X, Huang Z and Yin G. A novel akermanite/poly (lactic-co-glycolic acid) porous composite scaffold fabricated via a solvent casting-particulate leach-

ing method improved by solvent self-proliferating process. Regen Biomater 2017; 4: 233-242.
[26] Shuai CJ, Shuai CY, Feng P, Gao CD, Peng SP and Yang YW. Antibacterial capability, physicochemical properties, and biocompatibility of $nTiO_2$ incorporated polymeric scaffolds. Polymers (Basel) 2018; 10: 328.
[27] Zheng X, Zhang P, Fu Z, Meng S, Dai L and Yang H. Applications of nanomaterials in tissue engineering. RSC Adv 2021; 11: 19041-19058.
[28] Ramuta TZ, Starčič Erjavec M and Kreft ME. Amniotic membrane preparation crucially affects its broad-spectrum activity against uropathogenic bacteria. Front Microbiol 2020; 11: 469.
[29] Guo Q, Hao J, Yang Q, Guan L, Ouyang S and Wang J. A comparison of the effectiveness between amniotic membrane homogenate and transplanted amniotic membrane in healing corneal damage in a rabbit model. Acta Ophthalmol 2011; 89: E315-E319.
[30] Capistrano da Silva E, Carossino M, Smith-Fleming KM, Langohr IM and Martins BDC. Determining the efficacy of the bovine amniotic membrane homogenate during the healing process in rabbits' ex vivo corneas. Vet Ophthalmol 2021; 24: 380-390.
[31] Chen C and Kim WK. The application of micro-CT in egg-laying hen bone analysis: introducing an automated bone separation algorithm. Poult Sci 2020; 99: 5175-5183.
[32] Kim Y, Brodt MD, Tang SY and Silva MJ. MicroCT for scanning and analysis of mouse bones. Methods Mol Biol 2021; 2230: 169-198.
[33] Cochran DL, Oh TJ, Mills MP, Clem DS, McClain PK, Schallhorn RA, McGuire MK, Scheyer ET, Giannobile WV, Reddy MS, Abou-Arraj RV, Vassilopoulos PJ, Genco RJ, Geurs NC and Takemura A. A randomized clinical trial evaluating rh-FGF-2/beta-TCP in periodontal defects. J Dent Res 2016; 95: 523-530.
[34] Duruel T, Cakmak AS, Akman A, Nohutcu RM and Gumusderelioglu M. Sequential IGF-1 and BMP-6 releasing chitosan/alginate/PLGA hybrid scaffolds for periodontal regeneration. Int J Biol Macromol 2017; 104: 232-241.
[35] Li Y, Qiao Z, Yu F, Hu H, Huang Y, Xiang Q, Zhang Q, Yang Y and Zhao Y. Transforming Growth Factor-beta3/Chitosan Sponge (TGF-beta3/CS) facilitates osteogenic differentiation of human periodontal ligament stem cells. Int J Mol Sci 2019; 20: 4982.